Earth and Space Science

RESEARCH ARTICLE
10.1029/2021EA001861

Classification of GLM Flashes Using Random Forests

Jacquelyn Ringhausen[1], Phillip Bitzer[1], William Koshak[2], and John Mecikalski[1]

[1]Department of Atmospheric Science, University of Alabama in Huntsville, Huntsville, AL, USA, [2]Earth Science Branch, ST11, NASA Marshall Space Flight Center, Huntsville, AL, USA

Key Points:

- Although there is substantial overlap in the distributions for cloud-to-ground (CG) and intra-cloud (IC) flash characteristics, the mean values differ
- Most important features for flash distinction are maximum group area, time-of-day, elongation, propagation, footprint, slope, and max group/event distance
- Results show skill in the random forests model's ability to distinguish CG and IC flashes in the Geostationary Lightning Mapper data

Correspondence to:
J. Ringhausen,
jsr0013@uah.edu

Citation:
Ringhausen, J., Bitzer, P., Koshak, W., & Mecikalski, J. (2021). Classification of GLM flashes using random forests. *Earth and Space Science*, *8*, e2021EA001861. https://doi.org/10.1029/2021EA001861

Received 26 MAY 2021
Accepted 18 OCT 2021

Author Contributions:
Conceptualization: Jacquelyn Ringhausen, Phillip Bitzer
Formal analysis: Jacquelyn Ringhausen
Funding acquisition: Phillip Bitzer
Investigation: Jacquelyn Ringhausen
Methodology: Jacquelyn Ringhausen
Validation: Jacquelyn Ringhausen
Writing – original draft: Jacquelyn Ringhausen
Writing – review & editing: Phillip Bitzer, William Koshak, John Mecikalski

Abstract [The Geostationary Lightning Mapper (GLM) detects total lightning continuously from space, and does not distinguish intra-cloud (IC) from cloud-to-ground (CG) lightning. This research focuses on differentiating CG and IC lightning detected by GLM using a random forests (RF) model. GLM flash and group characteristics are implemented into the RF model and used to predict flash type. The most important flash characteristic for distinguishing flash type is the maximum group area. Other features with high feature importance include time-of-day, elongation, propagation, footprint, slope, maximum distance between groups and events, and mean energy. Skill scores showcase the model's ability to distinguish flash type with moderate skill, with 81% probability of detection, 71% percent correct, 36% false alarm rate, 36% false alarm ratio, and 56% critical success index. These scores improve further when study area is limited to CONUS and the Southeastern United States. These results can be used to aid in future climatological analysis of flash type.]

Plain Language Summary The Geostationary Lightning Mapper (GLM) is a satellite-based lightning sensor that allows for continuous detection of light emitted from the cloud tops due to lightning. GLM does not distinguish if the lightning is connecting to ground (CG) or remaining in the cloud (IC). In order to distinguish CG and IC flashes, this research uses a machine learning method called random forests (RF). The RF model attempts to classify lightning flashes based on their size, duration, and intensity. The most important flash characteristics for distinguishing flash type are the features related to the areal size of the lightning and the time of day the lightning occurs. Overall, moderate success is shown when attempting to divide total lightning into CG and IC over the 2018 period. This information can be used by researchers to improve the use of GLM in the study of different storm types as well as aiding in wildfire forecasting.

1. Introduction

Lightning is a natural phenomenon that can be used to provide insight into the severity of a storm (E. R. Williams et al., 1999; Goodman et al., 2005; Chronis et al., 2015; Schultz et al., 2015; W. J. Koshak et al., 2015), has been linked to the strengthening or weakening of a hurricane (Bovalo et al., 2014; Cecil et al., 2002; DeMaria et al., 2012; Fierro et al., 2011; Molinari et al., 1999; Ringhausen & Bitzer, 2021; Xu et al., 2017), and can cause damage to infrastructure and initiate devastating fires. Lightning is often classified into two main categories: cloud-to-ground (CG) lightning and intracloud (IC) lightning. These two lightning types relate differently to the dynamics and charge structure of a storm, and can signal different stages of storm development or strength (E. R. Williams et al., 1989). There also exists a third lightning type known as hybrid flashes, which possess attributes of IC lightning and also produce CG strokes to ground (R. M. Mecikalski et al., 2017). The distribution of flash type can change depending on storm type and location (Fuchs et al., 2015; R. M. Mecikalski & Carey, 2017). Thus, it is important to distinguish these lightning types in order to gain a detailed picture of storm dynamics in relation to lightning, which can aid in forecasting storm intensity. Being able to distinguish CG and IC lightning on a synoptic scale would allow for a climatological analysis of convective storm regimes, relationships to hail occurrence, and severe weather (Fuchs et al., 2015; Medici et al., 2017; Schultz et al., 2011).

The Geostationary Lightning Mappers (GLM) aboard the Geostationary Operational Environmental Satellites (GOES)-16 and 17 enable continuous monitoring of total lightning over land and ocean within the GOES-16 and 17 fields of view (FOV). GLM detects total lightning, however, there is no distinction made between IC and CG lightning within the GLM data. Ground-based networks such as the Earth Networks Total Lightning Network (ENTLN) and the National Lightning Detection Network (NLDN) do distinguish

lightning type, but more efficiently detect CG lightning relative to IC lightning (Cummins & Murphy, 2009). The detection efficiency (DE) of ground based networks varies spatially, decreasing over oceans and in areas with lower sensor density (Bitzer & Burchfield, 2016; Marchand et al., 2019; Rudlosky, 2014). GLM, alternatively, is better equipped for IC lightning detection and can detect lightning in data-sparse areas such as oceans and land areas where ground-based sensors are not as prominent. Thus, distinguishing between CG and IC lightning in the GLM data set could have significant impacts on determining in poorly observed areas where storms are strengthening or weakening (Schultz et al., 2011), where a hurricane is intensifying (Ringhausen & Bitzer, 2021), and where a wildfire is more likely to occur (Fairman & Bitzer, 2019).

The overall GLM DE shows large variation both spatially and temporally (Bateman et al., 2021; Cummins, 2021; Lapierre et al., 2017; Marchand et al., 2019; Murphy & Said, 2020; Rutledge et al., 2020; Zhang & Cummins, 2020). Past studies have shown GLM DE decreases with the increase of off-nadir viewing angle, which coincides with an increase in the minimum detectable optical energy threshold (Cummins, 2021; Marchand et al., 2019; Murphy & Said, 2020; Rudlosky & Virts, 2021). The spaced-based optical data are viewed in the form of events, groups, and flashes, where an event is an illuminated pixel, a group encompasses all adjacent events in the same frame, and a flash is composed of all groups that occur within a certain spatial and temporal threshold. Since CG groups are typically larger in area and optical energy, their detection will be less impacted by a higher energy threshold than IC groups, biasing GLM toward CG detection at large viewing angles. The GLM DE background threshold is also affected by the time-of-day. GLM DE is lower during the day because solar reflection from clouds and bodies of water increase the background illumination, which increases the minimum threshold for lightning detection (Cummins, 2021; Zhang & Cummins, 2020). Another potential impact on the GLM DE is regional and seasonal variations in storm type. GLM has been shown to have lower DE in storms with high flash rates such as anomalous storms (Murphy & Said, 2020; Rutledge et al., 2020). In general, it was found that the GLM flash DE increases with increasing flash duration, increasing flash area, and longer channel length (Rutledge et al., 2020; Zhang & Cummins, 2020).

Past research has made substantial contributions in showcasing differences in the flash characteristics of IC and CG lightning when looking at the space-based optical transient detector (OTD) and lightning imaging sensor (LIS) (W. J. Koshak, 2010; W. J. Koshak, 2011; W. J. Koshak & Solakiewicz, 2011). Analysis revealed that although there is substantial overlap in the two distributions, the mean values for the maximum group area (MGA) and maximum number of events in a group (MNEG) for CG and IC flashes statistically differ (W. J. Koshak, 2010). Based on these results, subsequent studies were able to retrieve an estimated ground flash fraction (i.e., the fraction of CG lightning to the total lightning) using the distributions of the means with minimal error (W. J. Koshak, 2011; W. J. Koshak & Solakiewicz, 2011). However, these methods did not provide a way to classify individual flashes. This was the motivation for a further study that introduced the analytic perturbation method (APM) for flash classification, which classified flashes in a simulation correctly over 78% of the time for LIS and OTD data (W. J. Koshak & Solakiewicz, 2015). APM still requires a large set of N lightning flashes, with APM errors increasing when $N < 2500$. Finally, a study by Rudlosky and Shea (2013) also showed differences in MGA (and MNEG) between CGs and ICs.

Applying all the OTD/LIS-based results to GLM, it is expected that CG lightning will have spatially larger GLM flash characteristics than IC lightning. Building on these past results, this study will use machine learning to differentiate CG and IC lightning in the GLM data using numerous group and higher-level flash characteristics in combination. We hypothesize that using a random forests (RF) model, GLM flashes will be able to be individually classified as CG or IC with moderate accuracy based on the flash characteristics alone.

To address the current lack of distinction between CG and IC lightning within the GLM data, we investigate how CG and IC lightning flashes appear optically from the perspective of GLM, and use GLM flash characteristics to distinguish lightning type. The main objective of this research is to generate a new application of GLM data through lightning type classification. In doing so, the purpose of this paper is to answer the following questions: (a) What are the differences in the GLM flash characteristics of CG and IC lightning? (b) Can these differences in flash characteristics be used to accurately classify CG and IC lightning flashes from GLM using machine learning?

Table 1
Results of Classification Accuracy (CA) Testing Broken Down by Pulse Type for Both Earth Networks Total Lightning Network (ENTLN) and National Lightning Detection Network (NLDN)

	ENTLN		NLDN	
Pulse type	Number of pulses	CA	Number of pulses	CA
First negative CG	72	93.1% (67/72)	71	98.6% (70/71)
First positive CG	16	87.5% (14/16)	16	93.8% (15/16)
All first CG	88	92% (81/88)	87	97.7% (85/87)
Subsequent negative CG	200	90.0% (180/200)	193	90.2% (174/193)
Subsequent positive CG	10	80.0% (8/10)	10	70.0% (7/10)
All subsequent CG	210	89.5% (188/210)	203	89.2% (181/203)
IC initial breakdown pulse	36	94.4% (34/36)	33	69.7% (23/33)
IC pulse	295	97.6% (292/295)	132	88.6% (117/132)
Preliminary breakdown pulse	30	100% (30/30)	19	100% (19/19)

2. Data and Methodology

This study uses a large data set with $N > 30{,}000{,}000$ GLM flashes for distinguishing between CG and IC lightning. The data spans 6 months from 2018, where months from each season were chosen to obtain a robust representation of the data. GLM data are sorted and grouped into three classifications: events, groups, and flashes (Goodman et al., 2013). An event is a single illuminated pixel that exceeds the background brightness threshold during a single frame. A group includes all adjacent events that occur in the same ~ 2ms frame. A flash consists of all groups that produce a Weighted Euclidian Distance of less than 1 within the bounds of 16.5km spatially and 330ms temporally (Goodman et al., 2010, 2013; Mach et al., 2007; Mach, 2020). We focus on the group and flash level GLM data in this research. Goodman et al. (2013) provides a full description of the GLM design.

Since we are working with GLM data from 2018, there are data processing issues that must be addressed before using the data to train the RF model. First, prior to October 15th, 2018 there is a GLM timing offset of approximately 123 ms caused by the unaccounted time it takes light to travel from cloud top to sensor (W. Koshak et al., 2018). This offset was accounted for prior to matching to the truth data set (ENTLN). Additionally, the GLM Level 2 (L2) data has an upper limit of 101 groups per flash, which can cause an unrealistic splitting of large flashes that contain more than 101 groups. This splitting of flashes could cause the distribution of CG and IC flashes to be unrepresentative. Peterson (2019) found that flash splitting occurs in around 5% of flashes, and cannot be ignored when looking at large amounts of data. Thus, flashes in this study have been resorted with no upper limit on the number of groups comprising a flash (Peterson, 2019).

2.1. Truth Data Set

A RF model requires training on a truth data set. Two ground-based very low frequency lightning datasets, NLDN and ENTLN, were considered to be the truth data set for flash classification. In order to choose between the two, a comparison from two days of data during the GOES-R field campaign in Huntsville, Alabama USA was performed to calculate the classification accuracy of each network. Lightning was classified by hand using the Huntsville Alabama Marx Meter Array data (Bitzer et al., 2013) and the North Alabama Lightning Mapping Array (Goodman et al., 2005) from April 22 and 27, 2017. Approximately 1,000 pulses (100 flashes) were used in this comparison. A pulse is defined as any lightning-related discharge (e.g., an IC discharge, a CG stroke, a preliminary breakdown pulse, or a narrow bipolar pulse). The results showed that NLDN did slightly better than ENTLN at classifying CG pulses (93.5% vs. 90.8%), while ENTLN did substantially better than NLDN at both detecting and classifying IC pulses (98.5% vs. 84.5% respectively) (Table 1). Based on these results and past findings (Zhu et al., 2017), ENTLN was chosen to be the truth data set for classification of GLM flashes.

The ENTLN is a worldwide lightning detection network operating between 1Hz and 12MHz (Liu et al., 2014). Sensors are not uniformly distributed worldwide, so DE varies geographically (Bitzer & Burchfield, 2016). ENTLN incorporates the World Wide Lightning Location Network (WWLLN) into its data set and has done so since December 2011, helping to improve DE over oceans (Rudlosky, 2014). In the ENTLN data set, pulses are sorted into flashes if they are within 700 ms and 10 km of another pulse. More information on ENTLN can be found in Liu et al. (2014).

2.2. Matching

A large data set consisting of GLM and ENTLN pulses and flashes from 2018 was assembled and matched at the pulse level, using spatial and temporal bounds of 32 km and 10 ms (Bitzer et al., 2016; Bitzer & Burchfield, 2016; Zhang et al., 2016). This matching is done to determine which measured ENTLN and GLM lightning detections are the result of the same discharge. A matched GLM flash is assigned as CG or IC based on the ENTLN classification. If multiple GLM groups are matched to an ENTLN pulse, the pair with the smallest time and spatial difference is matched. Similarly, if multiple GLM flashes match to an ENTLN flash, then the flash closest in time and space is used. If two flashes match within the bounds and one flash is closer in time, but another is closer in space, the flash closer in time is used. The entire GLM domain (54°N/S) is used in the matching and training of the RF model, but to limit misclassifications in the ENTLN data set, we also run the RF model with a more limited area encompassing the Continental U.S. (CONUS) and nearby coastal ocean within the bounds 20 to 50°N latitude and 125 to 65°W longitude. These bounds were chosen based on DE and classification accuracy of ENTLN, which substantially decreases outside of these bounds (Bitzer et al., 2016). To limit the results even further to an area where GLM DE has been shown to be least affected by off-nadir viewing angle (Cummins, 2021), we also run the RF model on a region of the Southeastern United States within the bounds of 30 to 35°N latitude and 90 to 80°W longitude. The RF results using these bounds will be compared to our training results for the larger GLM observational domain.

The GLM flash characteristics for each matched flash are used as input features to train the RF model to differentiate CG and IC lightning. There are 21 different spatial and temporal flash features listed in Table 2 that are used in the preliminary training of the model. These features were chosen and calculated based on past studies attempting to distinguish CG and IC flashes using OTD and LIS data (W. J. Koshak, 2010; W. J. Koshak & Solakiewicz, 2015) and new trends found in the GLM lightning data.

2.3. Random Forests Algorithm

This study uses a RF model (Breiman, 2001) for training and predicting flash type. A RF model was chosen due to its resistance to bias and overfitting when compared to other statistical models, as well as its proven usefulness in past weather prediction algorithms (J. K. Williams et al., 2008; Gagne et al., 2009; McGovern et al., 2011; Ahijevych et al., 2016; Herman & Schumacher, 2018b, 2018a; Medina et al., 2019; J. R. Mecikalski et al., 2021). Further, RF is capable of managing large data sets with high dimensionality such as the data set used in this research (N > 30,000,000) and can handle correlated features. RF is a tree-based classification technique that employs multiple decision trees consisting of numerous features of an observation and classifies it based on those features. RF can be classifiers (binary outcome), which is the case for our model, or regressors depending on what is being predicted. Decision trees are the building blocks of RF, and consist of maps of decisions with branches for each path. They are formulated on a series of yes/no questions (nodes) that utilize the predictors to best split the observations into their respective classifications. The result in the case of our model is a binary classification of CG or IC.

Hyperparameter optimization was performed using a grid search method to determine the ideal number of trees and node depth for the model to use (Probst et al., 2019). This method splits the training data set into n sets and trains on all but one (the validation set) using a list of provided values, then switches and trains on all but a different set, testing every combination n number of times. Using less than 200 trees causes the classification accuracy to decrease considerably, while using more than 200 trees does not substantially increase the probability of correct classification, but does increase the amount of time required for the model to run. Based on the results, 200 trees are chosen for the RF model with a maximum depth of 80 nodes. The data

Table 2
Definitions of Geostationary Lightning Mapper (GLM) Flash Characteristics Input as Features Into the Random Forests (RF) Model

Features	Definition
Spatial features	
Maximum group area	The maximum area associated with a single group in the flash
Maximum no. of events in a group	Maximum number of events associated with a single group in the flash
Footprint	The combined area of all the events comprising a flash
Propagation	Furthest separation of groups in a GLM flash divided by the diameter of the flash
Elongation	Furthest separation of events in a GLM flash divided by the diameter of the flash
Max distance between groups	Max distance between groups in a flash
Max distance between events	Max distance between events in a flash
Child count	Number of groups in a flash
Grandchild count	Number of events in a flash
Temporal features	
Time-of-day	Time of day in UTC
Time illuminated	Amount of time GLM groups were present in a flash
Duration	Time length of flash
Max time difference	Maximum amount of time between two subsequent groups
Number of contiguous groups	Number of groups that occur successively in time
Spatiotemporal/other features	
Slope	Max energy group in 2nd half minus max energy group in 1st half divided by time difference
Shape	Number of groups in first half of flash divided by total number of groups
Energy	Total additive energy of a flash
Maximum group energy	Maximum energy associated with a group in the flash
Mean energy	Average energy for all groups composing a flash
Standard dev. of energy	The standard deviation of energy for a flash
Energy threshold	Number of groups with an energy above the average group energy for the flash

was split into a training (75%: 25,767,185 flashes) and test (25%: 8,589,0610 flashes) data set. A classification prediction is given for each flash, and the results and skill scores calculated from a contingency table. Metrics used to determine the performance of the RF model include the probability of detection (POD), percent correct (PC), false alarm rate (FARate), false alarm ratio (FARatio, same as probability of false alarm) and the critical success index (CSI).

We determine the importance of individual flash features in the final prediction using feature importance (FI). FI is calculated using "Gini impurity" which is a measure of variance, or more specifically of how often a randomly chosen feature would be incorrectly classified if it was randomly labeled using the distribution of labels in the subset (Louppe et al., 2013). Each flash feature has a FI based on the number of branches or splits using a given feature weighted in proportion to the number of overall trees with that split (Friedman, 2001). Larger FI values mean the feature is more important in the classification outcome.

2.4. Predictive Features

There are 21 features used in the preliminary training of the model, which are defined in Table 2. Two unique features termed the slope and shape have been created to attempt to provide more detail about the

change in the shape and magnitude of the optical emission with time. Past observations of IC lightning have found that the number of large, medium, and small pulses differs throughout the duration of the flash (Bils et al., 1988; Shao & Krehbiel, 1996; Villanueva et al., 1994). Several studies found that the largest pulses occur at the beginning of an IC flash, while later stages of an IC flash are dominated by medium and small pulses (Bils et al., 1988; Villanueva et al., 1994). Since pulse amplitude and optical emission are intimately related, this suggests that for IC lightning the most energetic groups will occur earlier in the flash, and moderately less energetic groups later. However, the initial leader of an IC flash is typically lower in the cloud than pulses in the later stages of an IC flash, so the optical emission reaching cloud top (and the GLM sensor) will be similar between the two. In contrast, the most energetic part of a CG flash is the return stroke. A typical CG flash will have 3–5 return strokes, with mixed findings on whether the initial return stroke or the subsequent stroke is the most energetic (Nag et al., 2008). Regardless of which return stroke in a CG flash is the strongest, the difference in amplitude is likely to be much larger than for IC pulses, since IC pulses are weaker overall (Krider et al., 1980; Weidman & Krider, 1978, 1979). Thus, the energy difference between a group in the beginning of a CG flash and groups later in the flash is likely to be larger than the difference between IC groups. This is the motivation for the slope feature, which takes into account the maximum group energies (MGE) and their time, and is calculated using

$$slope = \frac{(MGE_2 - MGE_1)}{(t_2 - t_1)} \tag{1}$$

where MGE_1 and MGE_2 are the maximum energies associated with a group in the first and second half of the flash, respectively, and t_1 and t_2 are the times associated with those groups. Based on our earlier discussion of CG and IC lightning, it is expected that IC flashes will have positive slope values closer to zero, while CG flashes are more likely to have moderately large negative or positive slope values.

The shape feature deals with the number of groups rather than the energy. Just as the largest amplitude pulses occur earlier in an IC flash, a larger number of groups also occurs during the initial or active phase of an IC flash. This may seem counter-intuitive when looking at the overall number of pulses in some IC flashes (e.g., Figure 1a in Villanueva et al. (1994)). Even though there can sometimes be more pulses overall in the later stages of an IC flash, these pulses are typically smaller and will produce less optical emission than a larger pulse. Small pulses can have an additive effect when occurring in the same 2 ms timeframe to produce a GLM group, but often are not enough to overcome GLM thresholds. This is especially true for GLM when compared to LIS, since the GLM pixel size is much larger (Zhang & Cummins, 2020). Although more groups are also more likely to occur in the beginning of a CG flash (barring continuing current flashes), the ratio of the number of groups in the beginning half and end half of the flash is much smaller for a CG versus an IC flash. The shape feature is defined as

$$shape = \frac{N_1}{N}. \tag{2}$$

where N is the total number of groups in a flash, and N_1 is the total number of groups in the first half of the flash. Thus, we would expect larger shape values to be associated with IC flashes, and smaller values for CG flashes.

3. Results and Discussion

3.1. Trends in Flash Characteristics

Trends in flash characteristics show that IC and CG flashes tend to have similar numbers of groups composing them (Table 3). The number of events per flash, however, is larger on average for CG lightning versus IC lightning (86 vs. 63). Other spatial features show a similar trend, with the footprint, MGA, and MNEG all larger for CG flashes. Radiant energy features are also larger for CG flashes, including the energy, MGE, and mean energy.

Histograms of the data show clearly that there is substantial overlap between CG and IC flash characteristics (Figure 1). Even with this overlap, several features have preferred values for CG and IC flashes. For instance, a larger fraction of IC lightning have MGA values below 400 km^2, while a larger fraction of CG flashes have MGA values above 400 km^2. This same trend is present in the MNEG and flash footprints, with IC MNEG and footprints more often below 10 and 800 km^2 respectively, while CG flashes make up a large

Table 3
A Summary of the Mean, Median, and Standard Deviation for Each Feature According to Flash Type

	IC			CG		
Feature	Mean	Median	Stddev	Mean	Median	Stddev
Number of groups per flash	23.9	14.0	32.4	26.7	15.0	36.8
Number of events per flash	62.8	29.0	113.2	85.5	41.0	143.2
Footprint (km^2)	702.3	506.8	669.7	971.5	671.0	941.4
MGA (km^2)	470.8	300.1	470.8	681.4	431.1	732.5
MNEG	6.3	4.0	6.7	9.6	6.0	10.5
Energy (fJ)	388.4	138.9	959.6	566.4	195.3	1,332.3
Duration (ms)	389.4	322.0	321.5	420.5	346.0	347.2
Propagation	0.28	0.23	0.24	0.30	0.24	0.25
Elongation	0.64	0.65	0.30	0.71	0.74	0.29
Max dis. between groups (km)	395.3	8.5	974.1	329.9	8.2	907.3
Max dis. between events (km)	395.7	8.6	974.6	330.8	8.2	908.0
Time-of-day (local hour)	1,243	1,405	731	1,215	1,306	738
Time illuminated (sec)	0.15	0.10	0.17	0.16	0.10	0.18
Max time difference (sec)	0.116	0.106	0.074	0.122	0.111	0.077
Number of contiguous groups	4.8	3.0	6.5	5.6	3.0	7.8
Slope (fJ/s)	−64.6	2.7	5,298.7	−102.07	0.0	9,460.9
Shape	0.549	0.538	0.181	0.547	0.538	0.182
MGE (fJ)	71.5	33.6	143.9	116.3	47.3	233.4
Mean energy (fJ)	12.9	9.7	13.1	17.8	12.2	19.8
Standard dev. of energy	16.2	9.5	26.1	25.7	13.2	41.7
Energy threshold	0.208	0.125	0.222	0.194	0.111	0.212

Note. CG, cloud-to-ground; IC, intra-cloud; MGA, maximum group area; MGE, maximum group energy; MNEG, maximum number of events in a group.

fraction of the higher value bins. This means that CG flashes are more likely to be spatially larger than IC flashes. These trends are similar to those found in comparisons of CG and IC lightning detected by OTD/LIS data (Rudlosky & Shea, 2013; W. J. Koshak & Solakiewicz, 2015). The larger average CG flash characteristics are most likely due to the fact that CG flashes are more energetic on average than IC flashes and occur lower in the cloud, so the light has to travel further through the cloud, causing more scattering, and a more disperse region of light at the top of the cloud.

The slope values for CG flashes are on average larger than IC flashes, and this difference can be seen clearly in Figure 1g, where a larger percentage of the slope values closer to zero are IC flashes, supporting our use of the slope feature. Although the slope feature has some potential in distinguishing flash type, the shape feature was nearly the same on average for CG and IC flashes, and thus is not very useful in flash type distinction.

3.2. Feature Importance

One FI stands out among the rest: the MGA. This feature was shown to be important in distinguishing CG and IC lightning in past research with LIS and OTD (W. J. Koshak, 2010). According to the RF model, it is the most useful feature for GLM flash distinction (Figure 2). Another important feature for flash classification is the time-of-day. Although time-of-day is not directly a measurement of the lightning itself, it does point toward the tendency of lightning type to change with time-of-day and location. This is most likely due to preferential times for different storm types to occur (e.g., typical thunderstorms typically occur in the

10.1029/2021EA001861

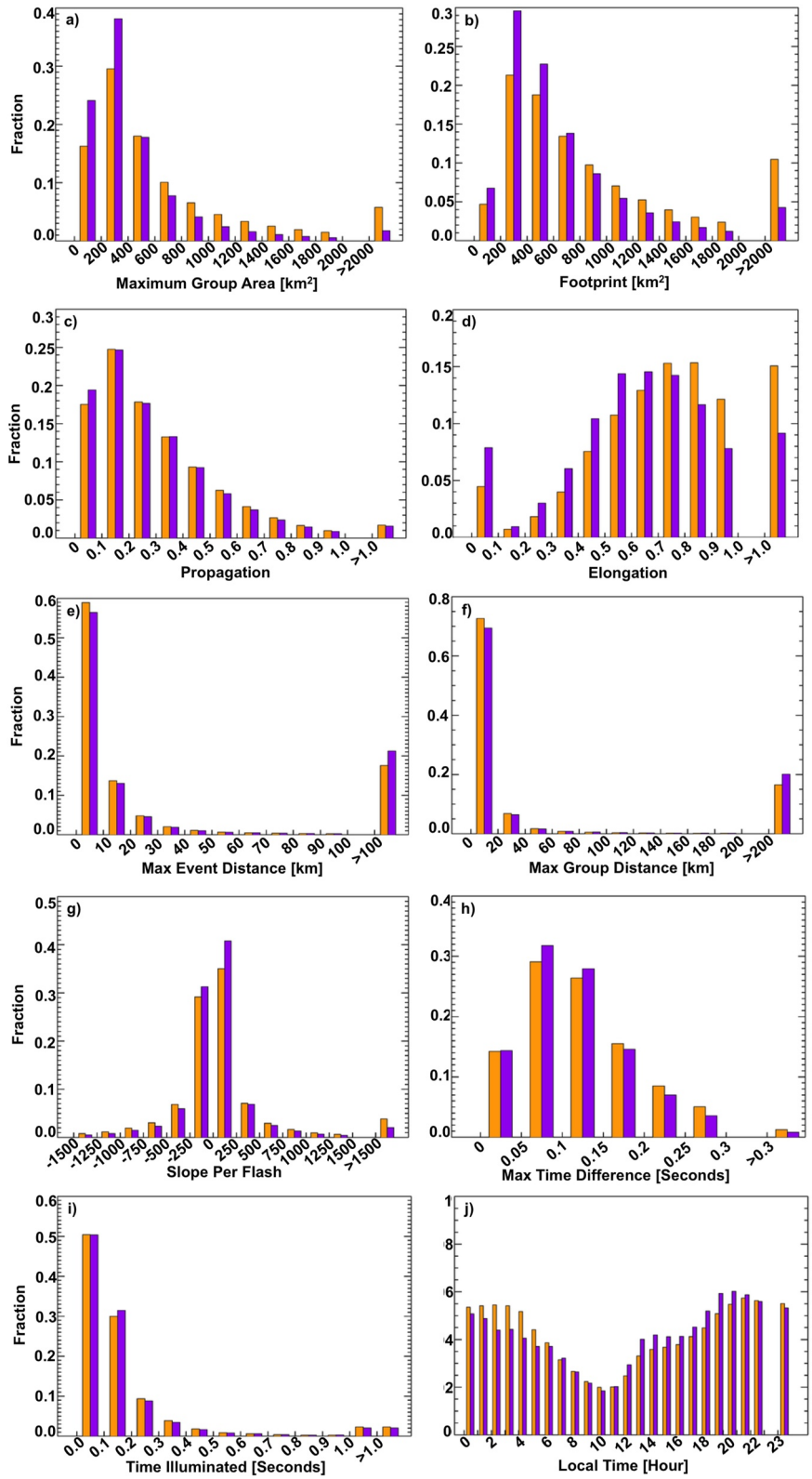

Figure 1. Histograms showing the distribution of cloud-to-ground and intra-cloud lightning flash characteristics for the top 10 most important features: (a) maximum group area, (b) footprint, (c) propagation, (d) elongation, (e) max group distance, (f) max event distance, (g) slope, (h) max time difference, (i) time illuminated, and (j) time-of-day. Yellow = CG, purple = IC.

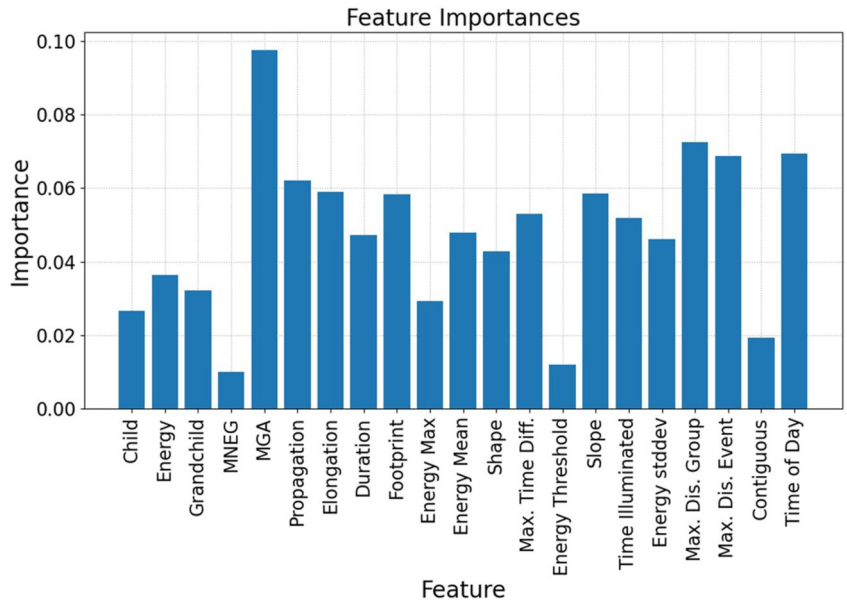

Figure 2. Feature importance for each lightning flash feature in the random forests model. MGA = maximum group area and MNEG = maximum number of events per group.

afternoon, while mesoscale convective systems occur overnight [Laing & Fritsch, 1997]) as well as certain locations favoring certain storm types. Thus, this feature can help pinpoint temporal environments favorable for CG versus IC lightning.

The next group of moderately important features for flash distinction are related to the shape of the lightning flash. These features include elongation, propagation, footprint, maximum distance between groups, maximum distance between events, and slope. Basically, CG flashes are more likely to be not only larger in area, but more elongated, i.e. more stretched in one direction versus the other. This could be influenced by horizontally extensive hybrid flashes in the data set being classified as CG flashes. Additionally, CG lightning is more energetic in general than IC lightning, but often occurs deeper in the cloud, so the light will have to pass through more cloud to escape from the top, causing more scattering, and thus a more disperse area of light for GLM to detect (Brunner & Bitzer, 2020).

The flash features with the lowest FI are most of the energy features including the overall flash energy, MGE, and the energy threshold. Energy features are less valuable in discerning flash types using RF, because although CG flashes are more energetic than ICs, they occur lower in the cloud, so less of the energy is reaching cloud top. IC flashes, on the other hand, occur higher in the cloud, so even though they are weaker, more of the energy reaches cloud top, causing the two lightning types to appear similar in energy at cloud top and as measured by GLM. The lowest ranked FI was the MNEG, which is most likely due to the high correlation between MGA and MNEG. When using Gini-impurity, the first of two highly correlated variables chosen as highly important will cause the other to be assigned a low FI. A few more features with lower FI include the grandchild and child count, as well as the number of contiguous groups. All of these features with lower FI can be removed from the model without greatly affecting the RF model's accuracy.

Table 4
The Number of Intra-Cloud and Cloud-to-Ground Flashes Used in the Training and Testing of the RF Model, and the Resulting Skill Scores

No. of matched flashes	Skill scores	Full FOV	CONUS	SE
CG.....12,351,487	POD	0.810	0.828	0.831
IC.....22,004,759	PC	0.714	0.748	0.746
Total....34,356,246	FARate	0.364	0.399	0.464
	FARatio	0.357	0.196	0.185
	CSI	0.562	0.689	0.699

Note. CSI, critical success index; FARate, false alarm rate; FARatio, false alarm ratio; PC, percent correct; POD, probability of detection; SE, Southeast.

3.3. Random Forests Model Results

The results of the classification of CG and IC flashes using the RF model show moderately high skills scores supporting a distinction in the flash characteristics of CG and IC lightning as viewed by GLM (Table 4). The RF model predictions produce a POD of 0.81 and a PC of 0.71, with a

FARate of 0.36, a FARatio of 0.36, and a CSI of 0.56. When using only data over CONUS, the skill scores improve, with substantial lowering in FARatio and a large increase in CSI. Further limiting the data to the Southeastern United States produces similar results as the RF model trained on CONUS. Lower ENTLN DE over the ocean and South America may be responsible for the decrease in skill when running the model using the full GLM FOV.

The most important feature in the model for distinguishing flash type is MGA, agreeing with past research findings (W. J. Koshak, 2010). Other useful features in predicting the correct flash type were the time-of-day, footprint, slope, elongation, propagation, time illuminated, maximum distance between events, maximum distance between groups, and the maximum time difference. In general, these results are promising for the potential use of GLM to classify CG and IC flashes.

4. Summary

This research investigates the differences between CG and IC lightning from an optical perspective and attempts to classify flashes based on their flash characteristics. A RF model is used to perform FI and lightning type classification. The main conclusions and answers to our original research questions are as follows:

1. Although there is substantial overlap in the distributions of CG and IC flash characteristics, there are differences in the means. On average, CG flashes are larger spatially than IC flashes from an optical perspective.
2. The most important feature in the correct prediction of flash type is the MGA, with CG flashes having larger MGA values on average when compared to IC flashes. Other important flash features in distinguishing flash type are the time-of-day, elongation, propagation, footprint, slope, maximum group and event distance, and energy mean. The least important features were the energy threshold, MNEG, the number of contiguous groups, and the grandchild count.
3. The RF model showed skill in distinguishing flash type, with a POD of 81%, a PC of 71%, a FARate of 36%, a FARatio of 36%, and a CSI of 56.2%. All skill scores improve when the data is limited to CONUS, with POD increasing to 83%, a PC of 75%, FARatio decreasing moderately to 20%, a FARate of 40%, and CSI increasing to 69%. The skill scores for the RF model trained on data limited to the Southeast display similar results to the CONUS trained RF model.

Some potential sources negatively affecting the RF model performance include the presence of hybrid flashes and instrumentation limitations. Hybrid flashes on average are larger in area and duration than CG or IC flashes alone (R. M. Mecikalski et al., 2017). Since all hybrid flashes in this study are classified as CG flashes, this would increase the overall spatial and temporal flash characteristic values for the CG flashes. GLM also has variation in its detection threshold, with an increasing minimum detectable energy threshold with distance from nadir (Cummins, 2021; Rutledge et al., 2020). This would cause less IC pulses to be detected off-nadir since ICs are less energetic overall than CGs, and would allow only the most energetic ICs to be detected, thus biasing the data set toward stronger IC pulses. All of these factors need to be taken into consideration for the future use of the RF model for lightning type classification.

In general, the results of this research are promising for the potential use of GLM to classify CG and IC flashes. Moving forward, data from additional years will be implemented into the model to see if these results are robust, specifically related to the potential influence of convective environmental changes associated with seasonally varying phenomena (e.g., monsoons, El Nino-La Nina). Future research will also investigate using separate models to account for regional and seasonal variability in lightning flash characteristics. Further, using our RF model, the cloud flash fraction over the entire FOV will be calculated and provide insights into storm type prevalence occurring in different regions including South America and the oceans where less is known about flash type prevalence.

Data Availability Statement

ENTLN data were provided by Earth Networks, and can be acquired by contacting Earth Networks: https://get.earthnetworks.com/contactus. GLM data for this study were obtained through the Comprehensive Large Array-Data Stewardship System (CLASS): https://www.avl.class.noaa.gov/saa/products/search?sub_id=0&datatype_family=GRGLMPROD&submit.x=31&submit.y=6.

Acknowledgments
This research was supported by the NOAA GOES-R Risk Reduction Research (R3) program.

References

Ahijevych, D., Pinto, J. O., Williams, J. K., & Steiner, M. (2016). Probabilistic forecasts of mesoscale convective system initiation using the random forest data mining technique. *Weather and Forecasting*, *31*(2), 581–599. https://doi.org/10.1175/waf-d-15-0113.1

Bateman, M., Mach, D., & Stock, M. (2021). Further investigation into detection efficiency and false alarm rate for the geostationary lightning mappers aboard goes-16 and goes-17. *Earth and Space Science*, *8*(2), e2020EA001237. https://doi.org/10.1029/2020EA001237

Bils, J. R., Thomson, E. M., Uman, M. A., & Mackerras, D. (1988). Electric field pulses in close lightning cloud flashes. *Journal of Geophysical Research*, *93*(D12), 15933–15940. https://doi.org/10.1029/JD093iD12p15933

Bitzer, P. M., & Burchfield, J. C. (2016). Bayesian techniques to analyze and merge lightning locating system data. *Geophysical Research Letters*, *43*, 12605–12613. https://doi.org/10.1002/2016GL071951

Bitzer, P. M., Burchfield, J. C., & Christian, H. J. (2016). A Bayesian approach to assess the performance of lightning detection systems. *Journal of Atmospheric and Oceanic Technology*, *33*(3), 563–5781. https://doi.org/10.1175/jtech-d-15-0032.1

Bitzer, P. M., Christian, H. J., Stewart, M., Burchfield, J., Podgorny, S., Corredor, D., et al. (2013). Characterization and applications of VLF/LF source locations from lightning using the Huntsville Alabama Marx Meter Array. *Journal of Geophysical Research*, *118*(8), 3120–3138. https://doi.org/10.1002/jgrd.50271

Bovalo, C., Barthe, C., Yu, N., & Bègue, N. (2014). Lightning activity within tropical cyclones in the south west indian ocean. *Journal of Geophysical Research: Atmospheres*, *119*(13), 8231–8244. https://doi.org/10.1002/2014jd021651

Breiman, L. (2001). Random forests. *Machine Learning*, *45*(1), 5–32. https://doi.org/10.1023/A:1010933404324

Brunner, K. N., & Bitzer, P. M. (2020). A first look at cloud inhomogeneity and its effect on lightning optical emission. *Geophysical Research Letters*, *47*(10), e2020GL087094. https://doi.org/10.1029/2020GL087094

Cecil, D. J., Zipser, E. J., & Nesbitt, S. (2002). Reflectivity, ice scattering, and lightning characteristics of hurricane eyewalls and rainbands. Part I: Quantitative description. *Monthly Weather Review*, *130*, 769–784. https://doi.org/10.1175/1520-0493(2002)130<0769:risalc>2.0.co;2

Chronis, T., Carey, L. D., Schultz, C. J., Schultz, E. V., Calhoun, K. M., & Goodman, S. J. (2015). Exploring lightning jump characteristics. *Weather and Forecasting*, *30*(1), 23–371. https://doi.org/10.1175/WAF-D-14-0006410.1175/WAF-D-14-00064.1

Cummins, K. L. (2021). On the spatial and temporal variation of GLM flash detection and how to manage it. In *10th conference on the meteorological application of lightning data, 101st annual meeting of the American Meteorological Society*.

Cummins, K. L., & Murphy, M. J. (2009). An overview of lightning locating systems: History, techniques, and data uses, with an in-depth look at the U.S. NLDN. *IEEE Transactions on Electromagnetic Compatibility*, *51*(3), 499–518. https://doi.org/10.1109/temc.2009.2023450

DeMaria, M., DeMaria, R. T., Knaff, J. A., & Molenar, D. (2012). Tropical cyclone lightning and rapid intensity change. *Monthly Weather Review*, *140*(6), 1828–18421. https://doi.org/10.1175/mwr-d-11-00236.1

Fairman, S. I., & Bitzer, P. M. (2019). Exploring the relationship between continuing current in lightning and lightning-initiated wildfires using the Geostationary Lightning Mapper. In *Agu fall meeting abstracts* (Vol. *2019*, 467 p. AE11A-3183).

Fierro, A. O., Shao, X.-M., Hamlin, T., Reisner, J. M., & Harlin, J. (2011). Evolution of eyewall convective events as indicated by intracloud and cloud-to-ground lightning activity during the rapid intensification of hurricanes Rita and Katrina. *Monthly Weather Review*, *139*(5), 1492–1504. https://doi.org/10.1175/2010MWR3532.1

Friedman, J. H. (2001). Greedy function approximation: A gradient boosting machine. *The Annals of Statistics*, *29*(5), 1189–1232. https://doi.org/10.1214/aos/1013203451

Fuchs, B. R., Rutledge, S. A., Bruning, E. C., Pierce, J. R., Kodros, J. K., Lang, T. J., et al. (2015). Environmental controls on storm intensity and charge structure in multiple regions of the continental United States. *Journal of Geophysical Research: Atmospheres*, *120*(13), 6575–6596. https://doi.org/10.1002/2015JD023271

Gagne, D. J., McGovern, A., & Brotzge, J. (2009). Classification of convective areas using decision trees. *Journal of Atmospheric and Oceanic Technology*, *26*(7), 1341–1353. https://doi.org/10.1175/2008jtecha1205.1

Goodman, S. J., Blakeslee, J. R., Koshak, W. J., Mach, D., Bailey, J., Buechler, D., et al. (2013). The GOES-R geostationary lightning mapper (GLM). *Elsevier*, *125–126*, 34–49. https://doi.org/10.1016/j.atmosres.2013.01.006

Goodman, S. J., Blakeslee, R., Christian, H., Koshak, W., Bailey, J., Hall, J., et al. (2005). The north Alabama lightning mapping array: Recent severe storm observations and future prospects. *Atmospheric Research*, *76*, 423–437. https://doi.org/10.1016/j.atmosres.2004.11.035

Goodman, S. J., Mach, D., Koshak, W., & Blakeslee, R. (2010). *GLM lightning cluster-filter algorithm (algorithm theoretical basis document)*. NOAA NESDIS Center for Satellite Applications and Research.

Herman, G. R., & Schumacher, R. S. (2018a). "Dendrology"in numerical weather prediction: What random forests and logistic regression tell us about forecasting extreme precipitation. *Monthly Weather Review*, *146*(6), 1785–1812. https://doi.org/10.1175/mwr-d-17-0307.1

Herman, G. R., & Schumacher, R. S. (2018b). Money doesn't grow on trees, but forecasts do: Forecasting extreme precipitation with random forests. *Monthly Weather Review*, *146*(5), 1571–1600. https://doi.org/10.1175/mwr-d-17-0250.1

Koshak, W., Mach, D., Bateman, M., Armstrong, P., & Virts, K. (2018). *Goes-16 GLM level 2 data full validation data quality* [product performance guide for data users].

Koshak, W. J. (2010). Optical characteristics of otd flashes and the implications for flash-type discrimination. *Journal of Atmospheric and Oceanic Technology*, *27*(11), 1822–1838. https://doi.org/10.1175/2010JTECHA1405.1

Koshak, W. J. (2011). A mixed exponential distribution model for retrieving ground flash fraction from satellite lightning imager data. *Journal of Atmospheric and Oceanic Technology*, *28*(4), 475–492. https://doi.org/10.1175/2010JTECHA1438.1

Koshak, W. J., Cummins, K. L., Buechler, D. E., Vant-Hull, B., Blakeslee, R. J., Williams, E. R., & Peterson, H. S. (2015). Variability of conus lightning in 2003-12 and associated impacts. *Journal of Applied Meteorology and Climatology*, *54*(1), 15–41. https://doi.org/10.1175/jamc-d-14-0072.1

Koshak, W. J., & Solakiewicz, R. J. (2011). Retrieving the fraction of ground flashes from satellite lightning imager data using conus-based optical statistics. *Journal of Atmospheric and Oceanic Technology*, *28*(4), 459–473. https://doi.org/10.1175/2010JTECHA1408.1

Koshak, W. J., & Solakiewicz, R. J. (2015). A method for retrieving the ground flash fraction and flash type from satellite lightning mapper observations. *Journal of Atmospheric and Oceanic Technology*, *32*(1), 79–961. https://doi.org/10.1175/JTECH-D-14-00085

Krider, E. P., Noggle, R. C., Pifer, A. E., & Vance, D. L. (1980). Lightning direction-finding systems for forest fire detection. *Bulletin of the American Meteorological Society*, *612*(9), 980–986. https://doi.org/10.1175/1520-0477(1980)061<0980:ldfsff>2.0.co;2

Laing, A. G., & Fritsch, M. (1997). The global population of mesoscale convective complexes. *Quarterly Journal of the Royal Meteorological Society*, *123*(538), 389–405. https://doi.org/10.1002/qj.49712353807

Lapierre, J. L., Stock, M., & Zhu, Y. (2017). Goes-16 geostationary lightning mapper comparison with the earth networks total lightning network. In (Vol. 2017, p. AE33A-2515). AA(Environmental Sciences, University of Virginia, Charlottesville, VA, United States Research and Development, Earth Networks Inc., Germantown, MD, United States), AB(Earth Networks Inc., German town, MD, United States), AC(University of Florida, Ft Walton Beach, FL, United States). Retrieved from https://ui.adsabs.harvard.edu/abs/2017AGUFMAE33A2515L

Liu, C., Sloop, C., & Heckman, S. (2014). *Application of lightning in predicting high impact weather*. 12410 Milestone Center Drive, Germantown, MAryland 20874.

Louppe, G., Wehenkel, L., Sutera, A., & Geurts, P. (2013). Understanding variable importances understanding variable importances in forests of randomized trees. *Advances in neural information processing systems*, *26*, 431–439. Retrieved from https://proceedings.neurips.cc/paper/4928-understanding-variable-importances-in-forests-of-randomized-trees.pdf

Mach, D. M. (2020). Geostationary lightning mapper clustering algorithm stability. *Journal of Geophysical Research: Atmospheres*, *125*(5), e2019JD031900. https://doi.org/10.1029/2019JD031900

Mach, D. M., Christian, H. J., Blakeslee, R. J., Boccippio, D. J., Goodman, S. J., & Boeck, W. L. (2007). Performance assessment of the optical transient detector and lightning imaging sensor. *Journal of Geophysical Research*, *112*(D9), D09210. https://doi.org/10.1029/2006JD007787

Marchand, M., Hilburn, K., & Miller, S. D. (2019). Geostationary lightning mapper and earth networks lightning detection over the contiguous United States and dependence on flash characteristics. *Journal of Geophysical Research: Atmospheres*, *124*(21), 11552–11567. https://doi.org/10.1029/2019JD031039

McGovern, A., John Gagne, D., II, Troutman, N., Brown, R. A., Basara, J., & Williams, J. K. (2011). Using spatiotemporal relational random forests to improve our understanding of severe weather processes. *Statistical Analysis and Data Mining: The ASA Data Science Journal*, *4*(4), 407–429. https://doi.org/10.1002/sam.10128

Mecikalski, J. R., Sandmæl, T. N., Murillo, E. M., Homeyer, C. R., Bedka, K. M., Apke, J. M., & Jewett, C. P. (2021). A random-forest model to assess predictor importance and nowcast severe storms using high-resolution radar–GOES satellite–lightning observations. *Monthly Weather Review*, *149*(6), 1725–1746.

Mecikalski, R. M., Bitzer, P. M., & Carey, L. D. (2017). Why flash type matters: A statistical analysis. *Geophysical Research Letters*, *44*(18), 9505–9512. https://doi.org/10.1002/2017GL0750033

Mecikalski, R. M., & Carey, L. D. (2017). Lightning characteristics relative to radar, altitude and temperature for a multicell, MCS and supercell over northern Alabama. *Atmospheric Research*, *191*, 128–140. https://doi.org/10.1016/j.atmosres.2017.03.001

Medici, G., Cummins, K. L., Cecil, D. J., Koshak, W. J., & Rudlosky, S. D. (2017). The intracloud lightning fraction in the contiguous United States. *Monthly Weather Review*, *145*(11), 4481–4499. https://doi.org/10.1175/MWR-D-16-0426.1

Medina, B. L., Carey, L. D., Amiot, C. G., Mecikalski, R. M., Roeder, W. P., McNamara, T. M., & Blakeslee, R. J. (2019). A random forest method to forecast downbursts based on dual-polarization radar signatures. *Remote Sensing*, *11*(7), 826. https://doi.org/10.3390/rs11070826

Molinari, J., Moore, P., & Idone, V. (1999). Convective structure of hurricanes as revealed by lightning locations. *Monthly Weather Review*, *127*, 520–534. https://doi.org/10.1175/1520-0493(1999)127<0520:csohar>2.0.co;2

Murphy, M. J., & Said, R. K. (2020). Comparisons of lightning rates and properties from the U.S. national lightning detection network (NLDN) and GLD360 with GOES-16 geostationary lightning mapper and advanced baseline imager data. *Journal of Geophysical Research: Atmospheres*, *125*(5), e2019JD031172. https://doi.org/10.1029/2019JD031172

Nag, A., Rakov, V. A., Schulz, W., Saba, M. M. F., Thottappillil, R., Biagi, C. J., et al. (2008). First versus subsequent return-stroke current and field peaks in negative cloud-to-ground lightning discharges. *Journal of Geophysical Research*, *113*(D19), D19112. https://doi.org/10.1029/2007JD009729

Peterson, M. (2019). Research applications for the geostationary lightning mapper operational lightning flash data product. *Journal of Geophysical Research: Atmospheres*, *124*(17–18), 10205–10231. https://doi.org/10.1029/2019jd031054

Probst, P., Wright, M. N., & Boulesteix, A.-L. (2019). Hyperparameters and tuning strategies for random forest. *WIREs Data Mining and Knowledge Discovery*, *9*(3), e1301. https://doi.org/10.1002/widm.1301

Ringhausen, J. S., & Bitzer, P. M. (2021). An in-depth analysis of lightning trends in hurricane Harvey using satellite and ground-based measurements. *Journal of Geophysical Research: Atmospheres*, *126*(7), e2020JD032859. https://doi.org/10.1029/2020JD032859

Rudlosky, S. D. (2014). Evaluating entln performance relative to TRMM/LIS. *Journal of Operational Meteorology*, *3*(2), 11–20.

Rudlosky, S. D., & Shea, D. T. (2013). Evaluating WWLLN performance relative to TRMM/LIS. *Geophysical Research Letters*, *40*(10), 2344–2348. https://doi.org/10.1002/grl.50428

Rudlosky, S. D., & Virts, K. S. (2021). Dual geostationary lightning mapper observations. *Monthly Weather Review*, *149*(4), 979–998. https://doi.org/10.1175/mwr-d-20-0242.1

Rutledge, S. A., Hilburn, K. A., Clayton, A., Fuchs, B., & Miller, S. D. (2020). Evaluating geostationary lightning mapper flash rates within intense convective storms. *Journal of Geophysical Research: Atmospheres*, *125*(14), e2020JD032827. https://doi.org/10.1029/2020JD032827

Schultz, C. J., Carey, L. D., Schultz, E. V., & Blakeslee, R. J. (2015). Insight into the kinematic and microphysical processes that control lightning jumps. *Weather and Forecasting*, *30*(6), 1591–16211. https://doi.org/10.1175/WAF-D-14-00147

Schultz, C. J., Petersen, W. A., & Carey, L. D. (2011). Lightning and severe weather: A comparison between total and cloud-to-ground lightning trends. *Weather and Forecasting*, *26*(5), 744–755. https://doi.org/10.1175/waf-d-10-05026.1

Shao, X. M., & Krehbiel, P. R. (1996). The spatial and temporal development of intracloud lightning. *Journal of Geophysical Research*, *101*(D21), 26641–26668. https://doi.org/10.1029/96JD01803

Villanueva, Y., Rakov, V. A., Uman, M. A., & Brook, M. (1994). Microsecond-scale electric field pulses in cloud lightning discharges. *Journal of Geophysical Research*, *99*(D7), 14353–14360. https://doi.org/10.1029/94JD01121

Weidman, C. D., & Krider, P. E. (1978). The fine structure of lightning return stroke waveforms. *Journal of Geophysical Research*, *83*(C12), 6239–6247. https://doi.org/10.1029/jc083ic12p06239

Weidman, C. D., & Krider, P. E. (1979). The radiation field wave forms produced by intracloud lightning discharge processes. *Journal of Geophysical Research*, *84*(C6), 3159–3164. https://doi.org/10.1029/jc084ic06p03159

Williams, E. R., Boldi, B., Matlin, A., Weber, M., Hodanish, S., Sharp, D., & Buechler, D. (1999). The behavior of total lightning activity in severe Florida thunderstorms. *Atmospheric Research*, *51*(3–4), 245–265. https://doi.org/10.1016/s0169-8095(99)00011-3

Williams, E. R., Weber, M. E., & Orville, R. E. (1989). The relationship between lightning type and convective state of thunderclouds. *Journal of Geophysical Research*, *94*(D11), 13213–13220. https://doi.org/10.1029/JD094iD11p13213

Williams, J. K., Ahijevych, D., Dettling, S., & Steiner, M. (2008). Combining observations and model data for short-term storm forecasting. *Proceedings of SPIE*, 708805. https://doi.org/10.1117/12.795737

Xu, W., Rutledge, S. A., & Zhang, W. (2017). Relationships between total lightning, deep convection, and tropical cyclone intensity change. *Journal of Geophysical Research: Atmospheres*, *122*(13), 7047–7063. https://doi.org/10.1002/2017jd027072

Zhang, D., Cummins, K., Nag, A., Murphy, M., & Bitzer, P. (2016). Evaluation of the national lightning detection network upgrade using the lightning imaging sensor. In *International lightning detection conference*.

Zhang, D., & Cummins, K. L. (2020). Time evolution of satellite-based optical properties in lightning flashes, and its impact on GLM flash detection. *Journal of Geophysical Research: Atmospheres*, *125*(6), e2019JD032024. https://doi.org/10.1029/2019JD032024

Zhu, Y., Rakov, V. A., Tran, M. D., Stock, M. G., Heckman, S., Liu, C., et al. (2017). Evaluation of ENTLN performance characteristics based on the ground-truth natural and rocket-triggered lightning data acquired in Florida. *Journal of Geophysical Research: Atmospheres*, *122*, 9858–9866. https://doi.org/10.1002/2017JD027270